

Strain Energy Release Rate of Double Cantilever Beam Specimen with Finite Thickness of Adhesive Layer

Kohei KOMATSU*, Hikaru SASAKI*
and Takamaro MAKU*

Abstract—Strain energy release rate G_I of DCB-FTAL (Double Cantilever Beam with Finite Thickness of Adhesive Layer) specimen was determined so as to include some variables as thickness and flexibility of adhesive layer and sizes and mechanical properties of adherend. For sharp crack case, the derived equation of G_I was compared with previous results, on the other hand, in case of thick adhesive layer, the derived equation of compliance C was compared with experimental results. Fracture Toughness G_{Ic} of DCB-FTAL specimen (Buna-Epoxy, EP-60 system) was also determined, and obtained results were discussed together with previous results.

Introduction

By now, a wide variety of experimental methods available for measuring Fracture Toughness (G_c or K_{Ic}) of materials has been established. One of the methods using a specimen of double cantilever beam (DCB) has been applied not only to the problem of fracture in homogeneous media¹⁾ but also to that in wood adhesive joint system^{2),**}. While there are some studies on the stress intensity factor for DCB specimen of homogeneous material by boundary collocation method^{3,4)} or finite element method⁵⁾, the study on fracture toughness of DCB specimen of wood adhesive joint has not been established well. Since the existence of finite thickness of adhesive layer makes difficulty of defining the stress distribution pattern at the vicinity of crack tip along the adhesive layer, compliance method⁶⁾ is thought easier for the approach to the fracture study of adhesive joint. In the compliance method, effort is needed to expressing the strain energy or the compliance of specimen as a function of the crack length and dimensions of specimen. For example, SASAKI** has expressed the compliance of DCB with finite thickness of adhesive layer (DCB-FTAL) specimen as shown in Fig. 1 as follows:

$$\delta/P=C=\frac{8}{E_x b} \left\{ \left(\frac{a+a_0}{h} \right)^3 + 0.3 \frac{E_x}{G_{xy}} \left(\frac{a}{h} \right) \right\}, \quad (1)$$

where, δ is opening distance at loading points, P is applied load, C is compliance, E_x

* Division of Composite Wood.

** SASAKI, H., Unpublished paper.

and G_{xy} ave modulus of elasticity and modulus of rigidity of adherend respectively, b and h are width and height of beam respectively. “ a ” is span of beam regarded as crack length. “ a_0 ” is called as off-set which was introduced to correct the rotations of cantilever beams at the fixed ends. By introducing this quantity a_0 , the behaviour of double cantilever beam with real span “ a ” and fixed imperfectly at the crack tip can be replaced by that of double cantilever beam with apparent span “ $a+a_0$ ” and fixed perfectly at the end of the apparent span. Sasaki obtained this quantity by comparing the eq. (1) with result of finite element analysis. It would be, however, troublesome in the sence of time and cost to determine the compliance or offset a_0 for each type of DCB-FTAL specimen with different thickness and flexibilities of adhesive layer by finite element method. It can be easily guessed that the compliance or a_0 is affected by the flexibility and thickness of adhesive layer as well as the elastic properties and geometric sizes of adherend. In this paper, the authors attempted to formulate the compliance of DCB-FTAL specimen so as to include the effects of the factors mentioned above.

Determination of Formula of Compliance

Opening distance δ at the loading points of DCB-FTAL specimen was determined by applying the theory of beam on the elastic foundation. In Fig. 2, the empirical deflection curve for the region-1 referred to bending moment is

$$v_1 = \frac{1}{E_x I} \left(\frac{Px^3}{6} + \frac{Pax^2}{2} + C_1x + C_2 \right), \tag{2}$$

where, I is moment of ineatia ($=bh^3/12$), C_1 and C_2 are constants of intergration to

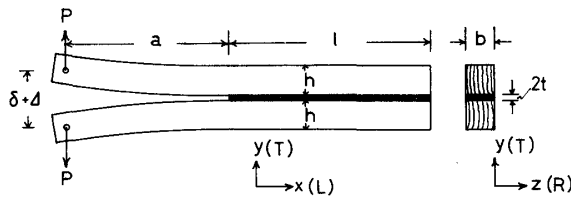


Fig. 1. DCB-FTAL specimen. L, R, T are longitudinal, radial and tangential direction of wood respectively. $\Delta = 2t + h$.

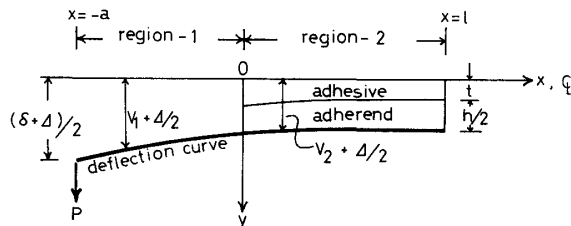


Fig. 2. Schematic relations for determining the compliance of DCB-FTAL specimen.

be determined in the next steps. In region-2, it is assumed that one of the adherends acts as a beam on the double layered elastic foundation. One of these two layers is adhesive layer of thickness t , and another is adherent layer of thickness $h/2$ as shown in Fig. 2. When this double layered elastic foundation which is regarded as the infinite rows of elastic springs are deflected by amount of v_2 , the reaction force per unit length of x direction acting on the deflection curve can be simply expressed as

$$q(x) = v_2(x) \left(\frac{E_y E_a}{k E_y + 0.5 E_a} \right) \left(\frac{b}{h} \right), \quad (3)$$

where, the ratio of $t = hk$ is introduced. In eq. (3) E_y is modulus of elasticity of adherend in y -direction, and E_a is modulus of elasticity of adhesive layer.

The basic differential equation of the beam subjected to the distributed load $-q(x)$ is

$$E_x I \frac{d^4 v_2}{dx^4} + q(x) = 0. \quad (4)$$

From eqs. (3), (4), we get

$$\frac{d^4 v_2}{dx^4} + 4\lambda^4 v_2 = 0, \quad (5)$$

where,

$$\lambda^4 = (E_y/E_x) (E_a/h^4) \left(\frac{3}{k E_y + 0.5 E_a} \right),$$

or

$$\frac{1}{\lambda h} = (E_x/E_y)^{0.25} \left\{ \frac{k(E_y/E_a) + 0.5}{3} \right\}^{0.25}. \quad (6)$$

The general solution of eq. (5) is

$$v_2 = e^{-\lambda x} (C_3 \cos \lambda x + C_4 \sin \lambda x) + e^{\lambda x} (C_5 \cos \lambda x + C_6 \sin \lambda x). \quad (7)$$

From the preliminary calculations, when a/h is larger than about 5, the term of $e^{\lambda x}$ in eq. (7) scarcely affects the value of compliance. Thus the constants of integration C_5 and C_6 can be neglected and $C_1 \sim C_4$ are determined from the following conditions.

$$v_1 = v_2, \quad \frac{dv_1}{dx} = \frac{dv_2}{dx}, \quad \frac{d^2 v_1}{dx^2} = \frac{d^2 v_2}{dx^2}, \quad \text{at } x=0$$

and

$$P - \int_0^{\infty} q(x) dx = 0. \quad (8)$$

Then we get

$$\begin{aligned} C_1 &= -\frac{P}{2\lambda^2} (1 + 2a\lambda), & C_2 &= \frac{P}{2\lambda^3} (1 + a\lambda), \\ C_3 &= \frac{P}{E_x I} \left(\frac{1}{2\lambda^3} + \frac{a}{2\lambda^2} \right), & C_4 &= -\frac{P}{E_x I} \left(\frac{a}{2\lambda^2} \right). \end{aligned} \quad (9)$$

Substituting C_1 and C_2 into eq. (2), the deflection curve of region-1 is

$$v_1(x) = \frac{P}{E_x I} \left\{ \frac{x^3}{6} + \frac{ax^2}{2} - \frac{(1 + 2a\lambda)x}{2\lambda^2} + \frac{1 + a\lambda}{2\lambda^3} \right\}. \quad (10)$$

The loading point deflection at $x=-a$ is

$$v_1(-a) = \frac{4P}{E_x b} \left\{ \left(\frac{a}{h} \right)^3 + 3 \left(\frac{1}{\lambda h} \right) \left(\frac{a}{h} \right)^2 + 3 \left(\frac{1}{\lambda h} \right)^2 \left(\frac{a}{h} \right) + 1.5 \left(\frac{1}{\lambda h} \right)^3 \right\}. \quad (11)$$

Considering the additional deflection by shear stress, the total opening distance δ at loading points of DCB-FTAL specimen is

$$\delta = \frac{8P}{E_x b} \left\{ \left(\frac{a}{h} \right)^3 + 3 \left(\frac{1}{\lambda h} \right) \left(\frac{a}{h} \right)^2 + \left[3 \left(\frac{1}{\lambda h} \right)^2 + 0.3 \left(\frac{E_x}{G_{xy}} \right) \right] \left(\frac{a}{h} \right) + 1.5 \left(\frac{1}{\lambda h} \right)^3 \right\}, \quad (12)$$

or

$$\frac{\delta}{P} = C = \frac{8}{E_x b} \left\{ \left(\frac{a}{h} + \frac{1}{\lambda h} \right)^3 + 0.3 \left(\frac{E_x}{G_{xy}} \right) \left(\frac{a}{h} \right) + 0.5 \left(\frac{1}{\lambda h} \right)^3 \right\}. \quad (13)$$

The final form of strain energy release rate G_I is obtained in accordance with the Irwin's equation⁶⁾ as

$$G_I = \frac{P^2}{2b} \frac{dC}{da} = \frac{P^2}{E_x b^2 h} \left\{ 12 \left(\frac{a}{h} + \frac{1}{\lambda h} \right)^2 + 1.2 \left(\frac{E_x}{G_{xy}} \right) \right\}. \quad (14)$$

On the other hand, the eq. (1) given by Sasaki leads the result similar to eq. (14) as

$$G_I = \frac{P^2}{E_x b^2 h} \left\{ 12 \left(\frac{a}{h} + \frac{a_0}{h} \right)^2 + 1.2 \left(\frac{E_x}{G_{xy}} \right) \right\}. \quad (15)$$

It is appeared by comparison of eq. (14) with eq. (15) that the off-set a_0 is externally equivalent to $1/\lambda$. Then in order to make sure of this relation, the following elastic constants of Mountain Ash (*Eucalyptus regnans* F. MUELL), with which Sasaki obtained a value of a_0 of DCB specimen, were substituted into eq. (6):

$$E_x = 24 \times 10^4, \quad E_y = 1.1 \times 10^4 \text{ (kg/cm}^2\text{)}.$$

The calculation of eq. (6) was done by putting $t=kh=0$ to coincide with the case of Sasaki. Thus,

$$\frac{1}{\lambda h} = 0.64 \left(\frac{E_x}{E_y} \right)^{0.25} = 1.383 \quad (16)$$

On the other hand, the value of a_0 given by Sasaki was

$$\frac{a_0}{h} = 1.4 \quad (17)$$

This may conclude that the off-set a_0 is equivalent to $1/\lambda$.

Comparison of Equation (14) with Previous Results in Case of Mathematically Sharp Crack.

In case of mathematically sharp crack, thickness of adhesive layer $2t$ is regarded as zero and the variable λ in eq. (14) takes the following form:

$$\frac{1}{\lambda h} = 0.64 \left(\frac{E_x}{E_y} \right)^{0.25}. \quad (18)$$

For the isotropic materials, Wiederhoh et al.³⁾ gave the stress intensity factor of DCB specimen by boundary collocation of two complex analytical functions as

$$K_I = \frac{Pa}{bh^{1.5}} \left\{ 3.467 + 2.315 \left(\frac{a}{h} \right) \right\}. \quad (19)$$

They reported that Gross and Srawley also gave an expression of K_I similar to eq. (19) by boundary collocation of William's⁷⁾ eigenfunction and that the first coefficient corresponding to eq. (19) was 3.46 and the second was 2.38**.

Walsh⁵⁾ also computed the stress intensity factor of DCB specimen of both isotropic and orthotropic materials by employing the calibrated finite element method and expressed K_I as follows:

$$K_I = \gamma \sigma \sqrt{a} \quad (\text{isotropic case}), \quad (20)$$

$$K_I = \beta \sigma \sqrt{a} \quad (\text{orthotropic case}), \quad (21)$$

$$\sigma = \frac{6P^*a}{h^2} \quad (P^* \text{ seems to be load per unit width, } P^* = P/b)$$

where, both γ and β are variable which change with a/h , and given for some values of a/h ⁵⁾.

Another formula of G_I of orthotropic DCB specimens is given by Okohira⁸⁾ as

$$G_I = \frac{P^2}{E_x b^2 h} \left\{ 12 \left(\frac{a}{h} \right) + 6.51 \frac{\alpha_I + \alpha_{II}}{\alpha_I \alpha_{II}} \left(\frac{a}{h} \right) + 1.2 \left(\frac{E_x}{G_{xy}} \right) + \left(\frac{1}{\alpha_I \alpha_{II}} - \mu_{xy} \right) \right\}. \quad (22)$$

In the formula, α_I and α_{II} are roots of following characteristic equation:

$$S_{22}\alpha^4 - (2S_{12} + S_{33})\alpha^2 + S_{11} = 0, \quad (23)$$

where,

$$\frac{1}{S_{11}} = E_x, \quad \frac{1}{S_{22}} = E_y, \quad \frac{1}{S_{33}} = G_{xy}, \quad \frac{1}{S_{12}} = -\frac{E_x}{\mu_{xy}}, \quad (23)$$

(in case of generalized plane stress),

and μ_{xy} is Poisson's ratio in xy-plane.

It is reported that eq. (22) was obtained by adding the deflection due to rotation at the fixed end to the empirical deflection formula of cantilever beam. The deflection caused by rotation was analyzed with the stress function of Fourier series by putting approximate boundary condition at the fixed ends as shown in Fig. 3.

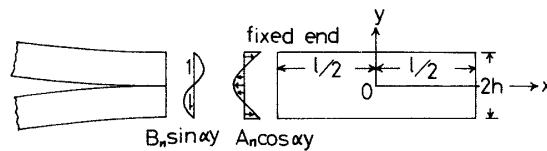


Fig. 3. Boundary conditions on the rectangular plate (from Okohira⁸⁾).

In order to examine the eq. (14), the equations (19), (20), and (21), which were expressed as the form of K_I , were transformed to the form of G_I through the following transform equation⁹⁾:

$$G_I = \frac{K_I^2}{E_x} \left(\frac{\alpha_I + \alpha_{II}}{2\alpha_I^2 \alpha_{II}^2} \right), \quad (24)$$

** See also Ref. 4).

where, α_I and α_{II} are roots of characteristic equation (23), and equal to unity for isotropic material. The reformed equations (19), (20), (21) and the original equations (14) and (22) are tabulated in Table 1. In numerical comparisons, 0.3 was taken as the Poisson's ratio of isotropic material, and the elastic constants of *Eucalyptus sieberi* were used for that of orthotropic material so as to coincide with Walsh's results⁵⁾ as

$$E_x=2.79, E_y=0.1395, G_{xy}=0.147, (\times 10^6 \text{ lb/in}^2) \mu_{xy}=0.5,$$

thus, $\alpha_I=0.9162, \alpha_{II}=0.2441$

Table 2 shows the values of function $F_n(a/h)$ for different values of a/h . It can be seen from this Table that eq. (14) is fairly good approximate expression even for

Table 1. Some equations of strain energy release rate G_I .

| Reference | general form... $G_I = \frac{P^2}{E_x b^2 h} F_n(a/h)$ |
|----------------------------------|--|
| Present work eq. (14) | $F_1(a/h) = 12(a/h + 1/\lambda h)^2 + 1.2 \frac{E_x}{G_{xy}}$ |
| Wiederhoh <i>et al.</i> eq. (19) | $F_2(a/h) = 12.02(a/h)^2 + 16.05(a/h) + 5.36$ |
| Walsh eq. (20) | $F_3(a/h) = 36\gamma^2(a/h)^3$ |
| Walsh eq. (21) | $F_4(a/h) = 36\beta^2(a/h)^3 \left(\frac{\alpha_I + \alpha_{II}}{2\alpha_I^2\alpha_{II}^2} \right)$ |
| Okohira eq. (22) | $F_5(a/h) = 12(a/h)^2 + 6.51 \frac{\alpha_I + \alpha_{II}}{\alpha_I\alpha_{II}}(a/h) + 1.2 \frac{E_x}{G_{xy}} + \left(\frac{1}{\alpha_I\alpha_{II}} - \mu_{xy} \right)$ |

Table 2. Values of function $F_n(a/h)$ for various values of a/h .

| a/h | Isotropic case | | | | Orthotropic case | | | |
|-------|----------------|------------|------------|----------|------------------|------------|------------|---------|
| | $F_1(a/h)$ | $F_2(a/h)$ | $F_3(a/h)$ | γ | $F_1(a/h)$ | $F_5(a/h)$ | $F_4(a/h)$ | β |
| 1.00 | 35.4 | 33.4 | | | 89.2 | 71.9 | | |
| 1.75 | 71.7 | 70.3 | 47.5 | 0.496 | 138.4 | 121.6 | 70.9 | 0.178 |
| 2.00 | 86.8 | 85.5 | | | 157.7 | 141.1 | | |
| 3.00 | 162.1 | 161.7 | | | 250.2 | 234.4 | | |
| 3.50 | 208.8 | 208.8 | 149.3 | 0.311 | 305.4 | 290.0 | 175.5 | 0.099 |
| 4.00 | 261.5 | 261.9 | | | 366.7 | 351.7 | | |
| 5.00 | 384.8 | 386.1 | | | 507.2 | 492.9 | | |
| 5.25 | 419.4 | 420.9 | 307.6 | 0.243 | 546.0 | 531.9 | 330.9 | 0.074 |
| 6.00 | 532.2 | 534.4 | | | 671.7 | 658.1 | | |
| 7.00 | 703.6 | 706.7 | 524.0 | 0.206 | 860.1 | 847.3 | 871.4 | 0.078 |
| 8.00 | 898.9 | 903.4 | | | 1072.6 | 1060.6 | | |
| 9.00 | 1118.3 | 1123.4 | | | 1309.1 | 1297.8 | | |
| 10.00 | 1361.6 | 1367.9 | | | 1569.6 | 1559.1 | | |

mathematically sharp crack and the results of finite element method incline to give a little smaller values than those of boundary collocation method or eqs. (14) and (22) except for $a/h=7$ in orthotropic material. The inclination that finite element analysis using the displacement method gives a little smaller values of K_I than those obtained by boundary collocation method was also noticed by Chan et al.¹⁰⁾ or Wilson¹¹⁾ who examined the effects of mesh size on the value of K_I .

Experimental

Specimen Preparation

Materials used in the present test are as follows. Adherend: Buna (Siebold's Beech, *Fagus crenata* **Bl.**). Adhesive: Epoxy resin which is a mixture of bis-phenol-A of WPE* 180~190 and di-butyl-phthalate plus 60 phr** of poly-sulfide as flexibilizer, and cured with 11 phr of di-ethylene-tri-amine at 20°C, 65% R.H. This type of epoxy adhesive containing 60 phr of flexibilizer is denoted as EP-60.

DCB-FTAL specimen shown in Fig. 1 was prepared in accordance with the Reservoir Method developed by Sasaki et al.¹²⁾. The span of cantilever beam "a" was varied from 3.5 cm to 12 cm at an interval of 0.5 cm. The thickness of adhesive layer $2t$ was prescribed by the teflon spacer shims of 0.15 cm and 0.30 cm thick. The height h and width b of single cantilever beam were 1.5 cm and 0.5 cm respectively. The total length of specimen $a+l$ was 18.5 cm long.

Mechanical Properties of Materials

In eq. (13) or eq. (14), it is clear that the most dominant factors on the value of compliance C or strain energy release rate G_I is the modulus of elasticity of adherend in x direction E_x . Therefore, E_x of Buna was measured by the three points bending test. The determination of E_x was based on the following equation¹³⁾.

$$E_x = \left(\frac{P}{\delta}\right) \left(\frac{1}{4b}\right) \left(\frac{L}{h}\right)^3 \left\{1 + 1.2 \left(\frac{E_x}{G_{xy}}\right) \left(\frac{h}{L}\right)^2\right\}, \quad (25)$$

where, P is applied load and δ is central deflection. b , h , and L are width, height, and span of beam respectively. The value of E_x/G_{xy} in this equation was taken as 17 which is a recommended value¹³⁾ for typical hard wood in Japan. Another mechanical properties were also adopted from appropriate references and listed in Table 3 together with the mean value of E_x of Buna.

Measurement of Compliance

Since the plastic deformation at the loading points of DCB-FTAL specimen was negligibly small comparing to the opening distance δ at loading points, the com-

* WPE : weight per epoxy equivalent.

** phr : parts per hundred of resin by weight.

Table 3. Mechanical properties of materials used in the present test.

| E_x (E_L) kg/cm ² | $E_x/E_y^{13)}$ (E_L/E_T) | $E_x/G_{xy}^{13)}$ (E_L/G_{LT}) | E_y/E_a (E_T/E_a) | E_a (1% strain) ¹²⁾ kg/cm ² |
|------------------------------------|-------------------------------|--|-------------------------|--|
| 90×10^3 | 21 | 17 | 1.7 | 2.5×10^3 |

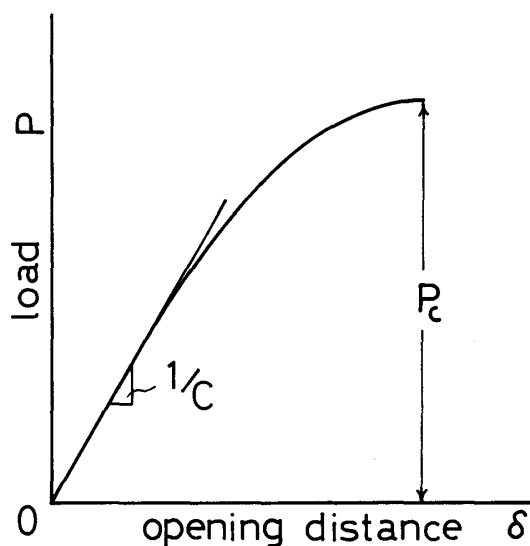


Fig. 4. Typical diagram of load-opening distance relation. P_c is fracture load. C is compliance determined on a linear portion of $P-\delta$ curve.

pliance of specimen was directly determined from the load deflection curve on the XY-recorder connected to the Instron type testing machine*. Fig. 4 shows a typical feature of the load-deflection curve. Nonlinear relation of load-deflection was observed when the adhesive layer was flexible and thick. This nonlinearity is not only brought from the material nonlinearity of adhesive and the plastic deformation at the vicinity of crack tip, but also partly caused by antiplane deflection of beam arms which might occur if configuration of specimen and loading condition were asymmetrical. Owing to this antiplane deflection, all of the energy supplied by movement of cross head was not necessarily consumed for increasing the reaction force P , hence nonlinear behaviour was amplified as deflection increase. Following to the definition of compliance, it will be incorrect to determine the compliance from this kind of indistinct test method. Almost all load-deflection curves had, however, a linear portion at low loading level, hence the compliance was determined approximately from the linear portion as shown in Fig. 4. The measurements were done at 20°C, 65% R.H. and constant cross head speed of 0.1 cm/min.

* TOM 200J Shinko Communication Ind. Ltd.

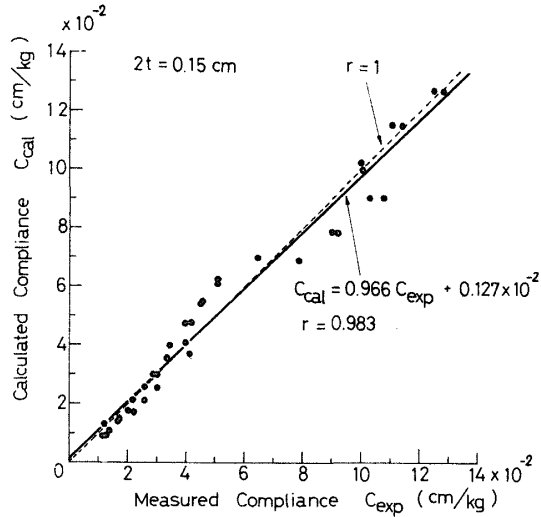


Fig. 5. Comparison of calculated compliance C_{cal} with measured compliance C_{exp} for $2t=0.15$ cm.

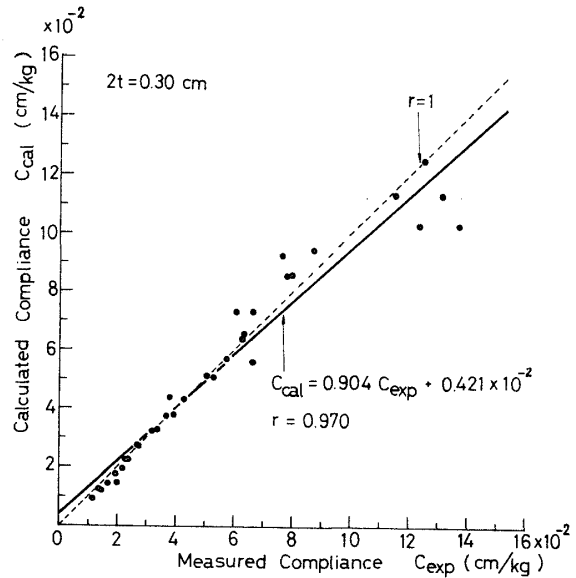


Fig. 6. Comparison of calculated compliance C_{cal} with measured compliance C_{exp} for $2t=0.30$ cm.

Results and Discussions

Fig. 5 and 6 show the comparison of measured compliance C_{exp} with calculated compliance C_{cal} , and Tables 4 and 5 show the individual test data and calculated results. By employing the least squares method, the following regression equations were obtained:

$$\text{for } 2t=0.15 \text{ cm, } C_{cal}=0.966C_{exp}+0.127 \times 10^{-2}, \quad r=0.983, \quad (26)$$

$$\text{for } 2t=0.30 \text{ cm, } C_{cal}=0.904C_{exp}+0.421 \times 10^{-2}, \quad r=0.970, \quad (27)$$

where, r is coefficient of correlation and $2t$ is thickness of adhesive layer. These results show that the nonlinearity of the load-deflection curves caused by material nonlinearity of adhesive layer and undesirable antiplane deflection of beam arms was more amplified as the thickness of adhesive layer increase. Therefore the better coincidence between experimental values C_{exp} and calculated results with eq. (13) C_{cal} was brought on $2t=0.15$ cm. Any way, it may conclude that the coincidence is not so bad for both case in consideration of the scatter of elastic constants in each specimen and inaccuracy at the determination of compliance.

Fig. 7 and 8 show the relation between fracture toughness G_{Ic} and crack length a . The calculation of G_{Ic} were done by substituting the fracture load P_e and dimensions of each specimen listed in Table 4 and 5 into eq. (14). It can be seen from Figs. 7 and 8 or Tables 4 and 5 that the values of G_{Ic} scatter considerably and seem to be somewhat dependent on the crack length, especially in case of $2t=0.30$ cm. This inclination may also be understood on the influence of the nonlinearity men-

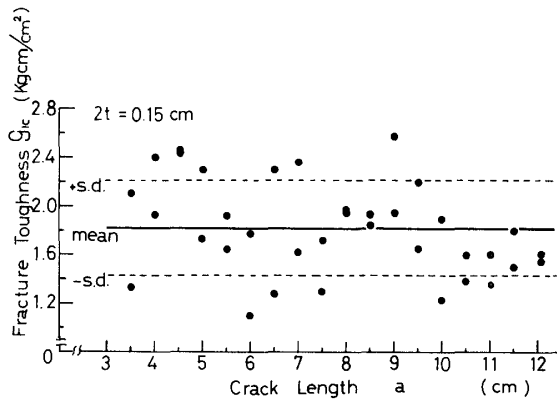


Fig. 7. Relationship between crack length a and Fracture Toughness G_{Ic} for $2t=0.15$ cm. s.d. means standard deviation.

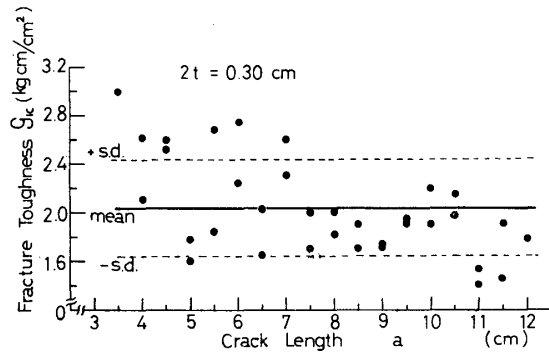


Fig. 8. Relationship between crack length a and Fracture Toughness G_{Ic} for $2t=0.30$ cm. s.d. means standard deviation.

tioned already in the discussions on the compliance. The influence of the nonlinearity is more evident in calculating G_{Ic} , because G_{Ic} is essentially determined from the fracture energy shown as

$$G_{Ic} = \frac{dU_c}{da}, \quad (28)$$

where, U_c is strain energy stored in the specimen from the beginning of loading till the fracture, i.e. $\int_0^\delta P(a, \delta) d\delta$.

For the nonlinear fracture behaviour, the estimation of G_{Ic} should be based on the eq. (28) as already tried by Liebowitz and Eftis¹⁴⁾. The aim of the present work, however, is to get a formula of compliance, hence the discussion for the nonlinear fracture behaviour of wood-adhesive joint system will be done in a separate paper.

As seen from Tables 4 and 5, the mean values of G_{Ic} obtained with eq. (14) are 1.82 kgcm/cm² with standard deviation of 0.39 kgcm/cm² for $2t=0.15$ cm and 2.04 kgcm/cm² with standard deviation of 0.40 kgcm/cm² for $2t=0.30$ cm. These values seem to be within reasonable range of G_{Ic} for flexible adhesive joint system comparing with the results by Sasaki²⁾ in which $G_{Ic}=0.96$ kgcm/cm² for $2t=0.15$ cm and $G_{Ic}=1.9$ kgcm/cm² for $2t=0.30$ cm in case of Mountain Ash-EP-60 system.

It can also be seen from the previous studies that the values of G_{Ic} obtained here are about one order of magnitude higher than those obtained for some kinds of solid wood^{15,16)} or wood adhesive joint systems in which the thickness of adhesive layer was negligibly thin^{17,*)} or rigidity of adhesive was very high^{2,**)}.

* KOMATSU, K., Unpublished data.

** TAKATANI, M., Unpublished data.

Table 4. Individual test data and calculated results for $2l=0.15$ cm.

| a cm | b^* cm | h^* cm | C_{exp} cm/kg $\times 10^{-2}$ | C_{cal} cm/kg $\times 10^{-2}$ | P_c kg | G_{Ic} kgcm/cm ² |
|--------------------|-------------|-------------|-------------------------------------|-------------------------------------|-------------|----------------------------------|
| 3.540 | 0.623 | 1.475 | 1.224 | 0.993 | 18.8 | 1.343 |
| 3.500 | 0.645 | 1.477 | 1.273 | 0.938 | 24.6 | 2.112 |
| 4.030 | 0.647 | 1.482 | 1.394 | 1.187 | 21.8 | 1.926 |
| 4.040 | 0.640 | 1.476 | 1.355 | 1.214 | 24.0 | 2.415 |
| 4.555 | 0.643 | 1.484 | 1.722 | 1.490 | 22.6 | 2.429 |
| 4.575 | 0.645 | 1.478 | 1.720 | 1.509 | 22.6 | 2.450 |
| 4.960 | 0.640 | 1.486 | 2.222 | 1.755 | 18.0 | 1.729 |
| 5.010 | 0.651 | 1.485 | 2.017 | 1.762 | 21.0 | 2.309 |
| 5.510 | 0.642 | 1.488 | 2.220 | 2.146 | 16.4 | 1.636 |
| 5.520 | 0.644 | 1.487 | 2.600 | 2.150 | 17.8 | 1.923 |
| 6.030 | 0.645 | 1.488 | 3.047 | 2.567 | 12.7 | 1.101 |
| 6.015 | 0.638 | 1.488 | 2.605 | 2.582 | 16.0 | 1.779 |
| 6.515 | 0.643 | 1.494 | 3.000 | 3.002 | 13.0 | 1.282 |
| 6.500 | 0.643 | 1.491 | 2.900 | 3.000 | 17.4 | 2.301 |
| 7.040 | 0.639 | 1.494 | 3.333 | 3.566 | 16.6 | 2.369 |
| 7.000 | 0.607 | 1.493 | 4.167 | 3.714 | 13.1 | 1.624 |
| 7.540 | 0.659 | 1.489 | 3.448 | 4.049 | 13.8 | 1.719 |
| 7.495 | 0.637 | 1.494 | 4.112 | 4.103 | 11.7 | 1.300 |
| 8.040 | 0.645 | 1.488 | 3.971 | 4.783 | 13.8 | 1.981 |
| 8.040 | 0.640 | 1.491 | 4.195 | 4.789 | 13.7 | 1.973 |
| 8.540 | 0.647 | 1.489 | 4.508 | 5.461 | 12.8 | 1.855 |
| 8.540 | 0.644 | 1.488 | 4.586 | 5.495 | 13.0 | 1.935 |
| 8.990 | 0.653 | 1.483 | 5.085 | 6.149 | 14.6 | 2.595 |
| 9.010 | 0.645 | 1.483 | 5.093 | 6.258 | 12.5 | 1.956 |
| 9.500 | 0.648 | 1.495 | 7.885 | 6.917 | 11.2 | 1.657 |
| 9.525 | 0.645 | 1.494 | 6.439 | 7.003 | 12.8 | 2.197 |
| 10.000 | 0.645 | 1.494 | 9.214 | 7.858 | 9.2 | 1.227 |
| 10.000 | 0.643 | 1.495 | 8.974 | 7.870 | 11.4 | 1.892 |
| 10.600 | 0.643 | 1.495 | 10.307 | 9.049 | 10.0 | 1.600 |
| 10.560 | 0.639 | 1.495 | 10.804 | 9.023 | 9.3 | 1.393 |
| 11.040 | 0.643 | 1.480 | 9.972 | 10.235 | 8.8 | 1.360 |
| 11.025 | 0.647 | 1.478 | 10.040 | 10.171 | 9.6 | 1.601 |
| 11.500 | 0.632 | 1.481 | 11.422 | 11.487 | 8.8 | 1.503 |
| 11.540 | 0.640 | 1.478 | 11.051 | 11.498 | 9.7 | 1.801 |
| 12.060 | 0.641 | 1.482 | 12.784 | 12.715 | 8.9 | 1.615 |
| 12.060 | 0.650 | 1.474 | 12.500 | 12.709 | 8.8 | 1.558 |
| mean value | | | | | | 1.818 |
| standard deviation | | | | | | 0.389 |

* mean value of measurements at 6~8 points per specimen.

Table 5. Individual test data and calculated results for $2t=0.30$ cm.

| a cm | b^* cm | h^* cm | C_{exp} cm/kg $\times 10^{-2}$ | C_{cal} cm/kg $\times 10^{-2}$ | P_c kg | C_{Ic} kgcm/cm ² |
|--------------------|-------------|-------------|-------------------------------------|-------------------------------------|-------------|----------------------------------|
| 3.520 | 0.647 | 1.475 | 1.173 | 0.979 | 29.0 | 3.014 |
| 4.040 | 0.640 | 1.475 | 1.486 | 1.254 | 22.2 | 2.115 |
| 4.045 | 0.648 | 1.475 | 1.400 | 1.242 | 25.0 | 2.620 |
| 4.450 | 0.641 | 1.480 | 1.708 | 1.482 | 23.0 | 2.525 |
| 4.435 | 0.640 | 1.483 | 2.077 | 1.469 | 23.4 | 2.600 |
| 5.040 | 0.630 | 1.473 | 2.157 | 1.924 | 16.6 | 1.613 |
| 4.900 | 0.639 | 1.472 | 1.982 | 1.799 | 18.0 | 1.780 |
| 5.540 | 0.635 | 1.487 | 2.228 | 2.273 | 20.4 | 2.689 |
| 5.500 | 0.630 | 1.476 | 2.325 | 2.274 | 16.8 | 1.846 |
| 6.080 | 0.640 | 1.474 | 2.689 | 2.751 | 19.4 | 2.746 |
| 6.045 | 0.641 | 1.470 | 2.648 | 2.730 | 17.6 | 2.250 |
| 6.530 | 0.631 | 1.470 | 3.208 | 3.258 | 15.6 | 2.034 |
| 6.500 | 0.614 | 1.470 | 3.379 | 3.316 | 13.7 | 1.646 |
| 7.000 | 0.621 | 1.479 | 3.935 | 3.790 | 15.4 | 2.311 |
| 7.000 | 0.633 | 1.468 | 3.686 | 3.780 | 16.8 | 2.601 |
| 7.500 | 0.635 | 1.472 | 4.268 | 4.354 | 14.2 | 2.031 |
| 7.525 | 0.628 | 1.475 | 3.769 | 4.414 | 12.9 | 1.714 |
| 8.065 | 0.628 | 1.473 | 5.018 | 5.167 | 12.6 | 1.821 |
| 8.000 | 0.628 | 1.471 | 5.263 | 5.090 | 13.4 | 2.042 |
| 8.560 | 0.641 | 1.483 | 5.709 | 5.704 | 12.0 | 1.707 |
| 8.500 | 0.640 | 1.487 | 6.600 | 5.584 | 12.8 | 1.914 |
| 9.055 | 0.640 | 1.478 | 6.310 | 6.552 | 11.6 | 1.762 |
| 9.000 | 0.639 | 1.479 | 6.283 | 6.461 | 11.6 | 1.748 |
| 9.575 | 0.652 | 1.479 | 6.076 | 7.315 | 11.8 | 1.915 |
| 9.510 | 0.645 | 1.473 | 6.609 | 7.348 | 11.8 | 1.956 |
| 10.070 | 0.641 | 1.463 | 7.986 | 8.603 | 11.0 | 1.920 |
| 10.025 | 0.644 | 1.456 | 7.836 | 8.571 | 11.8 | 2.201 |
| 10.535 | 0.643 | 1.483 | 7.600 | 9.245 | 11.5 | 2.164 |
| 10.540 | 0.646 | 1.467 | 8.750 | 9.459 | 10.9 | 1.984 |
| 11.000 | 0.637 | 1.487 | 12.373 | 10.287 | 9.3 | 1.536 |
| 11.045 | 0.647 | 1.484 | 13.730 | 10.280 | 9.0 | 1.411 |
| 11.500 | 0.645 | 1.487 | 13.115 | 11.319 | 8.9 | 1.476 |
| 11.575 | 0.646 | 1.496 | 11.508 | 11.312 | 10.2 | 1.922 |
| 12.040 | 0.644 | 1.498 | 12.500 | 12.457 | 9.5 | 1.784 |
| mean value | | | | | | 2.041 |
| standard deviation | | | | | | 0.397 |

* mean value of measurements at 6~8 points per specimen.

Conclusion

(1) The compliance of DCB-FTAL specimen was reasonably formulated so as to include some variables as thickness and flexibility of adhesive layer and sizes and mechanical properties of adherend by applying the theory of beam on elastic foundation.

(2) Though the eq.(13) was derived without considering the exact stress concentration at the vicinity of fixed ends of the beams, the applicability was fairly good even for the sharp crack case.

(3) Fracture of DCB-FTAL specimens was observed experimentally and the observed compliance coincided well with the calculated one with eq. (13).

(4) The Fracture Toughness G_{Ic} estimated with eq. (14) was about 2 kgcm/cm² for wood (Buna)-epoxy (EP-60) system, and this value was about 10 times of that for some kinds of solid wood or wood-adhesive joint system with negligibly thin adhesive layer or rigid adhesive layer.

References

- 1) For example, J. P. BERRY, J. Appl. Phys., **34**, (1) 62 (1963).
- 2) H. SASAKI, Setschaku (Adhesion & Adhesive) **18**, 172 (1974).
- 3) S. M. WIEDERHON, A. M. SHORB and R. L. MOSES, J. Appl. Phys., **39**, 1569 (1968).
- 4) J. E. SRAWLEY, B. GROSS, Materials Research & Standard, **7**, (4) 155 (1967).
- 5) P. F. WALSH, Eng. Fract. Mech., **4**, 533 (1972).
- 6) G. R. Irwin, Encyclopedia of Physics, **6**, 555 (1958).
- 7) M. L. WILLIAMS, J. Appl. Mech., **24**, 109 (1957).
- 8) Y. OKOHIRA, The Bulletin of the Faculty of Agriculture, Mie University., No. 47, 263 (1974).
- 9) R. H. LEICESTER, Techn. Paper of Div. For. Prod. CSIRO, Aust., No. 65 (1970).
- 10) S. K. Chan, I. S. Tuba and W. K. Wilson, Eng. Fract Mech., **2**, 1 (1970).
- 11) W. K. WILSON, Mechanics of Fracture 1, ed. by Shi, G. C., pp. 484 Noordhoff, Netherland (1973).
- 12) H. SASAKI, E. McArthar and J. W. GOTTSTEIN, For. Prod. J., **23**, 48 (1973).
- 13) Mokuzai Kogaku (Wood Technology), ed. by S. KAJITA, pp. 153 Yoken-Do, Japan (1961).
- 14) H. LEIBOWITZ and J. EFTIS, Eng. Fract. Mech., **3**, 267 (1971).
- 15) A. W. Porter, For. Prod. J., **14**, 325 (1964).
- 16) J. A. JOHNSON, Wood Science, **6**, 151 (1973).
- 17) K. L. W. HARISCHANDRA and Y. OKOHIRA, The Bulletin of the Faculty of Agriculture, Mie University, No. 49, 107 (1975).